Discrete Time-Frequency Characterizations of Dispersive Linear Time-Varying Systems

Ye Jiang and Antonia Papandreou-Suppappola

***Abstract*—A class of linear time-varying systems can be characterized by dispersive signal transformations, such as nonlinear shifts in the phase of the propagating signal, causing different frequencies to be shifted in time by different amounts. In this paper, we propose a discrete time-frequency model to decompose the dispersive system output into discrete dispersive frequency shifts and generalized time shifts, weighted by a smoothed and sampled version of the dispersive spreading function. The discretization formulation is obtained from the discrete narrowband system model through a unitary warping relation between the narrowband and dispersive spreading functions. This warping relation depends on the nonlinear phase transformations induced by the dispersive system. In order to demonstrate the effectiveness of the proposed discrete characterization, we investigate acoustic transmission over shallow water environments that suffers from severe degradations as a result of modal frequency dispersions and multipath fading. Using numerical results, we demonstrate that the discrete dispersive model can lead to a joint multipath-dispersion diversity that we achieve by properly designing the transmitted waveform and the reception scheme to match the dispersive environment characteristics.**

***Index Terms*—Discrete characterization, dispersive linear time-varying systems, diversity, frequency dispersion, matched signal transform, unitary warping, .**

I. Introduction

LINEAR TIME-VARYING (LTV) systems can be represented in terms of the transformations they induce on the propagation signal. For example, a narrowband LTV system can delay all time and frequency components of the transmitted signal by fixed amounts. As a result, the received signal from a narrowband LTV system has been described as a superposition of constant time and frequency shifts, weighted by the narrowband spreading function [1]–[3]. When the narrowband assumptions are not valid, wideband LTV systems are characterized by time shifts and Doppler scale changes, instead of constant frequency shifts, to describe the effect of the system on the transmitted signal [4]–[7].

Dispersive[1] LTV systems can cause different frequencies to be shifted in time by different amounts [6], [8]–[10]. Such dispersive signal transformations are specific to the nature of the system or environment that the signal propagates through. These transformations can be characterized by the nonlinear change $\xi(t/t_r)$ in the phase function of the signal, where $t_r > 0$ is a reference time point. For example, in a shallow water acoustic environment, the phase of the signal has been shown to change according to $\xi(t/t_r) = \sqrt{(t/t_r)^2 - (\alpha/t_r)^2}$, $t \gg \alpha$ [8], [9]. Also, the dispersive propagation of a shock wave through a steel beam follows $\xi(t/t_r) = \sqrt{t/t_r}$, $t > 0$ [11]. Other examples of dispersive systems include dielectric mediums (e.g., white light through a prism), radio waves in the ionosphere, trans-ionospheric signals measured by satellites [12], and acoustical waves reflected from a spherical shell immersed in water [13]. In such scenarios, characterizations using the narrowband spreading function do not provide accurate representations of the dispersive changes. Instead, matched spreading functions that depend on $\xi(t/t_r)$ need to be employed to provide a pointwise measure of how the transmission energy spreads in the time-frequency plane [6]. As a result, a dispersive system output can be modeled as a superposition of dispersive signal transformations, weighted by this matched dispersive spreading function.

The aforementioned spreading function system representations, although accurate, are generally difficult to analyze and impractical to implement as they are based on continuous signal transformations. Alternative discrete formulations have been developed for narrowband system characterizations [14], [15]. Specifically, a discrete narrowband time-frequency model decomposes the narrowband spreading function representation into a weighted summation of sampled time-frequency shifts, weighted by a smoothed discrete version of the spreading function [16], [17]. Such a discrete characterization has proven useful in many narrowband processing applications. For example, it can effectively exploit joint Doppler-multipath diversity from a fast fading, frequency-selective wireless channel to significantly increase system performance [17], [18]. It can also eliminate the need for complicated methods of estimating actual (often dynamic) parameters; estimation of these parameters reduces to estimating the expansion coefficients of time-frequency shifted signal terms [19]. Recently, a time-scale model was developed as a discrete characterization of wideband time-varying systems [7], [20], [21]. This model was shown to be useful in achieving joint multipath-scale diversity over wideband wireless channels by properly designing the signaling and reception schemes using wavelet techniques [20]. Similar to narrowband and wideband processing, dispersive system processing can benefit from a well-structured, discrete characterization, but such a framework has not yet been developed.

In this paper, we propose a discrete characterization of dispersive LTV systems as a generalization of the discrete

Manuscript received November 16, 2005; revised June 5, 2006. This work was supported in part by the National Science Foundation under CAREER Award CCR-0134002 and in part by the Department of Defense under Grant AFOSR FA9550-05-1-0443. The associate editor coordinating the review of this manuscript and approving it for publication was Prof. Fredrik Gustafsson.

The authors are with the Department of Electrical Engineering, Arizona State University, Tempe, AZ 85287-7206 USA (e-mail: jiangye@asu.edu; papandreou@asu.edu).

Color versions of one or more of the figures in this paper are available online at http://ieeexplore.ieee.org.

Digital Object Identifier 10.1109/TSP.2006.890916

[1]By the use of the term *dispersive systems*, we follow the definition from underwater acoustics [8] to refer to systems causing nonlinear signal transformations where, for example, high frequencies may be shifted by smaller amounts in time than low frequencies. This is different from the use of dispersive channels in the communications literature.

narrowband time-frequency model. Specifically, the dispersive spreading function representation is decomposed in terms of sampled dispersive frequency shifts and generalized time shifts, weighted by a smoothed discrete version of the dispersive spreading function. We base the discretization on a unitary warping relation between narrowband and dispersive LTV systems that depends on the function $\xi(t/t_r)$ [6]. Thus, by properly choosing the function $\xi(t/t_r)$, our proposed approach unifies the discretization procedure for any dispersive system through a unitary warping relation between the narrowband spreading function and the dispersive spreading function. The function $\xi(t/t_r)$ also specifies the sampling intervals that are associated with the finite time and frequency supports of the dispersively transformed signals.

In order to demonstrate the applicability of the discrete dispersive time-frequency model, we consider acoustic transmission over shallow water environments that suffers from severe degradation as a result of modal frequency dispersions and multipath fading. Historically, multipath has been considered as a source of diversity to increase performance [22]. However, no effort has been made to reduce the degradation by exploiting frequency dispersion. Thus, we introduce the concept of a joint *multipath-dispersion diversity* offered by the dispersive shallow water environment based on the proposed discrete dispersive spreading function representation. Furthermore, we investigate the problem of designing matched transmitted waveform and reception schemes to achieve this inherent diversity for use with wideband direct sequence spread spectrum techniques. We also develop a generalized time-frequency RAKE receiver structure that exploits the joint multipath-dispersion diversity. We demonstrate, via illustrative examples, that our proposed model can remarkably outperform conventional systems that are based on narrowband models.

The paper is organized as follows. In Section II, we review the discrete narrowband system characterization. We then discuss dispersive systems and their warping relation to narrowband systems in Section III. In Section IV, we derive the discretization model, and, in Section V, we demonstrate the advantage of our proposed model for shallow water acoustic transmissions.

II. Narrowband System Characterization and Discrete Processing

Narrowband LTV system representations can be generalized to characterize dispersive LTV systems by applying matched time-frequency warping transformations. Thus, we first review the discrete representation of narrowband LTV systems as it provides the underlying framework for deriving the discrete representation for dispersive systems.

For a linear operator $\mathcal{L}$ on $L_2(\mathbb{R})$ corresponding to a narrowband system, the narrowband spreading function (SF) is defined as [23]

$$\mathrm{SF}_{\mathcal{L}}(\tau,\nu)=\int_{-\infty}^{\infty} K_{\mathcal{L}}\left(t+\frac{\tau}{2},t-\frac{\tau}{2}\right)\mathrm{e}^{-j2\pi t\nu}dt.$$

The operator kernel $K_{\mathcal{L}}(t,\tau)$ can be considered as the time-varying impulse response of the narrowband LTV system as the output signal $(\mathcal{L}x)(t)$ can be represented in terms of the input signal $x(t)$ using $(\mathcal{L}x)(t)=\int_{-\infty}^{\infty}K_{\mathcal{L}}(t,\tau)x(\tau)d\tau$. Using the SF, the output of a narrowband LTV system can be interpreted as a weighted superposition of time-frequency shifted versions of the input signal[2]

$$(\mathcal{L}x)(t)=\int_{-\infty}^{\infty}\int_{-\infty}^{\infty}\mathrm{SF}_{\mathcal{L}}(\tau,\nu)\mathrm{e}^{-j\pi\tau\nu}(\mathcal{M}_{\nu}\mathcal{S}_{\tau}x)(t)d\nu d\tau. \quad (1)$$

The frequency shift and time shift on the signal are given, respectively, by[3]

$$(\mathcal{M}_{\nu}x)(t)=x(t)\mathrm{e}^{j2\pi\nu t} \quad (2)$$

$$(\mathcal{S}_{\tau}x)(t)=x(t-\tau). \quad (3)$$

Thus, the SF acts as a weighting function that quantifies the scattering strength at a constant time shift τ and frequency shift ν in (1). These shifts are constant in the sense that, for example, the frequency shift ν is not dependent on the analysis time. This is because the change in the phase of the signal, νt in (2), caused by the nondispersive system $\mathcal{L}$ in (1), is linear, and, thus, the resulting frequency shift given by the derivative of the phase is constant.

A discrete representation form of (1) in terms of sampled time shifts and sampled frequency shifts for the narrowband LTV system was developed by Bello [15] based on signal time and bandwidth constraints. A similar formulation was also obtained in [17], [18] in order to design the transmission signaling and to achieve full multipath and Doppler diversity. Specifically, if $x(t)$ is bandlimited in frequency to $[f_0,f_1]$ with bandwidth $W=f_1-f_0$, and $(\mathcal{L}x)(t)$ is time limited to $[t_0,t_1]$, with time duration $T=t_1-t_0$, then (1) can be written as

$$(\mathcal{L}x)(t)=\sum_{l\in\mathbb{Z}}\sum_{k\in\mathbb{Z}}\widehat{\mathrm{SF}}_{\mathcal{L}}(l/W,k/T)\left(\mathcal{M}_{\frac{k}{T}}\mathcal{S}_{\frac{l}{W}}x\right)(t). \quad (4)$$

The 2-D values of the smoothed SF are sampled at the uniform grid $\tau=l/W$ and $\nu=k/T$, and are given by

$$\widehat{\mathrm{SF}}_{\mathcal{L}}(\tau,\nu)=\int_{-\infty}^{\infty}\int_{-\infty}^{\infty}\mathrm{SF}_{\mathcal{L}}(\tilde{\tau},\tilde{\nu})\mathrm{e}^{-j\pi\tilde{\nu}\tilde{\tau}}\mathrm{e}^{-j\pi(\nu-\tilde{\nu})(t_0+t_1)}$$
$$\times\mathrm{e}^{j\pi(\tau-\tilde{\tau})(f_0+f_1)}\cdot\mathrm{sinc}\left((\nu-\tilde{\nu})T\right)\mathrm{sinc}\left((\tau-\tilde{\tau})W\right)d\tilde{\nu}d\tilde{\tau} \quad (5)$$

where $\mathrm{sinc}(x)=\sin(\pi x)/(\pi x)$. If the SF has bounded support $(\tau,\nu)\in[\tau_0,\tau_1]\times[\nu_0,\nu_1]$, the sampling intervals in (4) can be bounded as[4] $\lfloor\tau_0W\rfloor\le l\le\lceil\tau_1W\rceil$ and $\lfloor\nu_0T\rfloor\le k\le\lceil\nu_1T\rceil$.

[2]Note that (1) could be used to also represent wideband, dispersive, or any other physical system. This is because, for any arbitrary physical system that can be modeled as a Hilbert–Schmidt operator (in this case, an LTV system with square integrable 2-D impulse response), the representation in (1) can be applied with the Heisenberg group structured unitary operators $\mathcal{M}$ and $\mathcal{S}$, independent of the underlying physical model. However, the resulting spreading function $\mathrm{SF}(\tau,\nu)$, for a dispersive system, for example, will be a complicated mathematical function as (1) will be a mismatched representation. A different choice of spreading function with matched unitary operators will have a more concentrated support region.

[3]The signal transformation operators used in this paper are summarized in Table I.

[4]Note that $\lfloor x\rfloor$ ($\lceil x\rceil$) rounds x to the integer nearest to zero (infinity).

TABLE I
FREQUENTLY USED OPERATORS IN THE PAPER

Notation	Operator Name	Effect of the operator on a signal
$\mathcal{F}$	Fourier transform	$(\mathcal{F}x)(f) = X(f) = \int_{-\infty}^{\infty} x(t)e^{-j2\pi ft}dt$
$\mathcal{F}^{-1}$	Inverse Fourier transform	$(\mathcal{F}^{-1}X)(t) = x(t) = \int_{-\infty}^{\infty} X(f)e^{j2\pi ft}df$
$\mathcal{S}_{t_0}$	Time-shift	$(\mathcal{S}_{t_0}x)(t) = x(t-t_0)$
$\mathcal{M}_{f_0}$	Frequency-shift	$(\mathcal{M}_{f_0}x)(t) = x(t)e^{j2\pi tf_0}$
$\mathcal{D}_{\beta}^{(\xi)}$	Dispersive frequency-shift	$(\mathcal{D}_{\beta}^{(\xi)}x)(t) = x(t)e^{j2\pi\beta\xi(\frac{t}{t_r})}$
$\mathcal{G}_{\zeta}^{(\xi)}$	Dispersive time-shift	$\sqrt{\frac{\xi'(\frac{t}{t_r})}{\xi'\ \xi^{-1}\ \xi(\frac{t}{t_r})-\zeta}}\left(t_r\xi^{-1}\left(\xi(\frac{t}{t_r})-\zeta\right)\right)$
$\mathcal{H}_{\beta} = \mathcal{D}_{\beta}^{(\xi_{\ln})}$	Hyperbolic frequency-shift	$(\mathcal{H}_{\beta}x)(t) = x(t)\,e^{j2\pi\beta\ln\frac{t}{t_r}},\ t>0$
$\mathcal{U}_{\xi}$	Dispersive warping in time	$(\mathcal{U}_{\xi}x)(t) = \frac{1}{\sqrt{\lvert\xi'(\xi^{-1}(\frac{t}{t_r}))\rvert}}\,x(t_r\xi^{-1}(\frac{t}{t_r}))$

III. DISPERSIVE LTV SYSTEM CHARACTERIZATION

When a signal undergoes dispersive transformations while propagating through a medium, the SF will not, in general, be the appropriate analysis tool. This is because the dispersive transformation results in different frequency shifts depending on the processing time. To accurately characterize a dispersive system, it is important to incorporate its dispersive characteristics into the system representation.

A. Dispersive Spreading Function

If a dispersive system $\mathcal{Z}$ changes the phase function of the input signal $x(t)$ by $\xi(t/t_r)$, the dispersive (time-dependent) frequency shift is given by $\nu(t) = (d/dt)\xi(t/t_r)$. Thus, an appropriate system representation must involve this characteristic function $\xi(t/t_r)$. The dispersive SF (DSF) was developed to match the system dynamics based on this characteristic function in [6]. Specifically, the DSF, $\mathrm{DSF}_{\mathcal{Z}}(\zeta,\beta)$, was used to interpret the system output $(\mathcal{Z}x)(t)$ as a weighted superposition of dispersive transformations on $x(t)$

$$(\mathcal{Z}x)(t) = \int_{-\infty}^{\infty}\int_{-\infty}^{\infty} \mathrm{DSF}_{\mathcal{Z}}(\zeta,\beta)\mathrm{e}^{-j\pi\zeta\beta}\left(\mathcal{D}_{\beta}^{(\xi)}\mathcal{G}_{\zeta}^{(\xi)}x\right)(t)d\zeta d\beta. \tag{6}$$

These transformations correspond to a dispersive frequency shift operation

$$\left(\mathcal{D}_{\beta}^{(\xi)}x\right)(t) = \left(\mathcal{U}_{\xi}^{-1}\mathcal{M}_{\beta/t_r}\mathcal{U}_{\xi}x\right)(t) = x(t)\mathrm{e}^{j2\pi\beta\xi(t/t_r)} \tag{7}$$

and a generalized time shift operation

$$\left(\mathcal{G}_{\zeta}^{(\xi)}x\right)(t) = \left(\mathcal{U}_{\xi}^{-1}\mathcal{S}_{t_r\zeta}\mathcal{U}_{\xi}x\right)(t) \tag{8}$$

where the parameters ζ and β are dimensionless. Note that the operations in (7) and (8) are unitarily related to the frequency shift operation $(\mathcal{M}_{\beta/t_r}x)(t)$ in (2) and the time shift operation $(\mathcal{S}_{t_r\zeta}x)(t)$ in (3), respectively. The unitary warping operator $\mathcal{U}_{\xi}$ in (7) and (8) is defined as

$$(\mathcal{U}_{\xi}x)(t) = \left|t_r\xi'\left(\xi^{-1}(t/t_r)\right)\right|^{-1/2} x\left(t_r\xi^{-1}(t/t_r)\right) \tag{9}$$

where $(\mathcal{U}_{\xi}^{-1}\mathcal{U}_{\xi}x)(t) = x(t)$. The warping relationship assumes that $\xi(t/t_r)$ is a one-to-one function with $\xi'(t/t_r) = (d/dt)\xi(t/t_r)$ and $\xi^{-1}(\xi(t/t_r)) = t/t_r$. Note that techniques to implement this nonlinear warping transformation have been presented in [24]–[26]. The representation in (6) corresponds to a dispersive system that is, indeed, linear. This follows since, as the operation $(\mathcal{M}_{\beta/t_r}\mathcal{S}_{t_r\zeta}x)(t)$ is linear, its unitarily equivalent operation $(\mathcal{D}_{\beta}^{(\xi)}\mathcal{G}_{\zeta}^{(\xi)}x)(t) = (\mathcal{U}_{\xi}^{-1}\mathcal{M}_{\beta/t_r}\mathcal{S}_{t_r\zeta}\mathcal{U}_{\xi}x)(t)$ is also linear.

Depending on $\xi(t/t_r)$, the formulation in (6) can simplify to a specific system characterization. For example, when $\xi(t/t_r) = \ln(t/t_r)$, the system output can be represented as a weighted superposition of hyperbolic frequency shifts and scale changes [6], [27]. The latter follows since (8) simplifies to dilation/compression signal transformations. When $\xi(t/t_r) = \sqrt{(t/t_r)^2 - (\alpha/t_r)^2}$ and $t \gg \alpha$, the system in (6) corresponds to a shallow water acoustic environment causing dispersive frequency shifts in (7) and approximate time shifts in (8) (see Section V).

B. Unitary Warping Relations

Unitary warping methods have played an important role in matching signal or system dispersive characteristics [6], [10], [28]. For example, narrowband LTV system representations can be generalized to characterize dispersive LTV systems by applying matched time-frequency warping transformations. Specifically, the DSF associated with a dispersive system $\mathcal{Z}$ can be obtained as the narrowband SF associated with the warped system $\mathcal{U}_{\xi}\mathcal{Z}\mathcal{U}_{\xi}^{-1}$ [16], i.e.,

$$\mathrm{DSF}_{\mathcal{Z}}(\zeta,\beta) = \mathrm{SF}_{\mathcal{U}_{\xi}\mathcal{Z}\mathcal{U}_{\xi}^{-1}}(t_r\zeta,\beta/t_r). \tag{10}$$

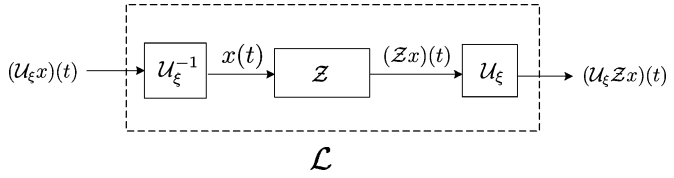

Fig. 1. Warping relation between the dispersive system $\mathcal{Z}$ and the unitary equivalent narrowband system $\mathcal{L} = \mathcal{U}_\xi \mathcal{Z} \mathcal{U}_\xi^{-1}$.

This warping relation is depicted in Fig. 1, where the input and output of the dispersive system $\mathcal{Z}$ are $x(t)$ and $(\mathcal{Z}x)(t)$, respectively. The composite system $\mathcal{U}_\xi \mathcal{Z} \mathcal{U}_\xi^{-1}$ is a unitary equivalent narrowband system [6], for which the input and output are the time warped signals $(\mathcal{U}_\xi x)(t)$ and $(\mathcal{U}_\xi \mathcal{Z}x)(t)$, respectively. Following (1), this equivalent narrowband system $\mathcal{U}_\xi \mathcal{Z} \mathcal{U}_\xi^{-1}$ can be characterized by its spreading function

$$(\mathcal{U}_\xi \mathcal{Z}x)(t) = \int_{-\infty}^{\infty}\int_{-\infty}^{\infty} \mathrm{SF}_{\mathcal{U}_\xi \mathcal{Z} \mathcal{U}_\xi^{-1}}(\tau,\nu) \times \mathrm{e}^{-j\pi\tau\nu} (\mathcal{M}_\nu \mathcal{S}_\tau \mathcal{U}_\xi x)(t) d\nu d\tau. \quad (11)$$

IV. Discrete Dispersive System Characterization

In order to formulate a discrete characterization of dispersive LTV systems based on the DSF representation, we first introduce the concept of a matched signal transform. This is an important transform as it generalizes the Fourier transform to match dispersive characteristics; also, the support of the propagating signal in this transform domain affects the discrete model. Our proposed discretization is derived from the existing discrete SF representation by utilizing the unitary warping relation between the SF and DSF. The dispersive discrete model can be useful in many applications. For example, as we will demonstrate, it can facilitate waveform design to improve reception performance by exploiting an inherent diversity in shallow water acoustic transmissions.

A. Matched Signal Transforms

As we have seen in Section III, the dispersive environment is characterized by the change in phase $\xi(t/t_r)$ of the transmitted waveform in (7). The matched signal transform (MST) is a linear transform that highly localizes signals with phase $\xi(t/t_r)$. For a given $\xi(t/t_r)$, the MST of $x(t)$ is defined as [10]

$$\aleph_x^{(\xi)}(\lambda) = \int_{t\in\wp} \sqrt{|\xi'(t/t_r)|}\, x(t) \mathrm{e}^{-j2\pi\lambda\xi\left(\frac{t}{t_r}\right)} dt \quad (12)$$

where $\lambda \in \mathbb{R}$ and $\wp$ is the domain of $\xi(t/t_r)$. Table II provides some MSTs for analyzing different types of signals by choosing the function $\xi(t/t_r)$.

The MST is highly localized for signals whose phase function matches $\xi(t/t_r)$. Specifically, the MST of a generalized chirp $g(t)$ yields a Dirac delta function at the rate λ_0 of the chirp

$$g(t) = \sqrt{|\xi'(t/t_r)|}\, \mathrm{e}^{j2\pi\lambda_0\xi\left(\frac{t}{t_r}\right)} \Rightarrow \aleph_g^{(\xi)}(\lambda) = \delta(\lambda-\lambda_0). \quad (13)$$

Therefore, the MST generalizes the Fourier transform as it is highly localized in the same way that sinusoids are localized by the Fourier transform. This follows since the Fourier transform $(\mathcal{F}y)(f)$ of the warped signal $y(t) = (\mathcal{U}_\xi x)(t)$ in (9) is the MST of $x(t)$ up to an axis scaling; that is

$$\begin{aligned}(\mathcal{F}\mathcal{U}_\xi x)(f) &= \int_{-\infty}^{\infty} (\mathcal{U}_\xi x)(t) \mathrm{e}^{-j2\pi f t} dt \\ &= \int_{t\in\wp} \sqrt{|\xi'(t/t_r)|}\, x(t) \mathrm{e}^{-j2\pi f t_r \xi\left(\frac{t}{t_r}\right)} dt \\ &= \aleph_x^{(\xi)}(f t_r). \end{aligned} \quad (14)$$

B. Discrete Dispersive Time-Frequency Model and Finite Approximations

Recall from Section III that the output signal $(\mathcal{Z}x)(t)$ of a dispersive LTV system $\mathcal{Z}$ with characteristic function $\xi(t/t_r)$ and an input signal $x(t)$ is given by (6). Next, we propose a discrete formulation of (6) based on sampling the dispersive frequency shift and generalized time shift parameters in (7) and (8), respectively.

We first assume that the MST of $x(t)$ in (12), $\aleph_x^{(\xi)}(\lambda)$, has a bounded support $\lambda \in [\lambda_0, \lambda_1]$, with an effective width $\Lambda = \lambda_1 - \lambda_0$. This is a reasonable assumption as the MST is well matched to changes in phase by $\xi(t/t_r)$. We also assume that the time warped signal $(\mathcal{U}_\xi \mathcal{Z}x)(t)$ has a bounded time support $t \in [t_r\gamma_0, t_r\gamma_1]$, with a normalized duration $\Gamma = \gamma_1 - \gamma_0$. Then, the output $(\mathcal{Z}x)(t)$ in (6) can be expressed as the weighted summation

$$(\mathcal{Z}x)(t) = \sum_{l\in\mathbb{Z}}\sum_{k\in\mathbb{Z}} \widehat{\mathrm{DSF}}_{\mathcal{Z}}(l/\Lambda, k/\Gamma) x_{l,k}(t) \quad (15)$$

where

$$x_{l,k}(t) = \left(\mathcal{D}_{k/\Gamma}^{(\xi)} \mathcal{G}_{l/\Lambda}^{(\xi)} x\right)(t) \quad (16)$$

are discrete dispersive frequency-shifted and generalized time-shifted versions of the input signal $x(t)$ as in (7) and (8). The weighting coefficients $\widehat{\mathrm{DSF}}_{\mathcal{Z}}(l/\Lambda, k/\Gamma)$ are 2-D samples of a smoothed version of the DSF given by

$$\begin{aligned}\widehat{\mathrm{DSF}}_{\mathcal{Z}}(\zeta,\beta) = \int_{-\infty}^{\infty}\int_{-\infty}^{\infty} \mathrm{DSF}_{\mathcal{Z}}(\tilde{\zeta},\tilde{\beta}) \mathrm{e}^{-j\pi(\beta-\tilde{\beta})(\gamma_0+\gamma_1)} \\ \cdot \mathrm{e}^{j\pi(\zeta-\tilde{\zeta})(\lambda_0+\lambda_1)} \mathrm{sinc}\left((\beta-\tilde{\beta})\Gamma\right) \mathrm{sinc}\left((\zeta-\tilde{\zeta})\Lambda\right) d\tilde{\zeta} d\tilde{\beta}. \end{aligned} \quad (17)$$

The summations in (15) also admit a finite approximation due to physical constraints of the dispersive system. Specifically, if the DSF is nonzero only when $(\zeta,\beta) \in [\zeta_0,\zeta_1] \times [\beta_0,\beta_1]$, the weighting coefficients $\widehat{\mathrm{DSF}}_{\mathcal{Z}}(l/\Lambda, k/\Gamma)$ in (17) are significantly nonzero only when the smoothing function's mainlobe supports, $[(l-1)/\Lambda, (l+1)/\Lambda]$ and $[(k-1)/\Gamma, (k+1)/\Gamma]$, are effectively overlapped with $[\zeta_0,\zeta_1]$ and $[\beta_0,\beta_1]$, respectively. Thus, the summation limits are determined as $\lfloor \zeta_0\Lambda \rfloor \le l \le \lceil \zeta_1\Lambda \rceil$ and $\lfloor \beta_0\Gamma \rfloor \le k \le \lceil \beta_1\Gamma \rceil$.

C. Discretization Procedure

We present next the procedure of sampling the dispersive frequency shift and generalized time shift parameters to obtain the

TABLE II
MST EXAMPLES BASED ON THE WARPING FUNCTION $\xi(t/t_r)$

$\xi(t/t_r)$	MST $\aleph_x^{(\xi)}(c)$	Transform
t/t_r	$X(c/t_r)=\int_{-\infty}^{\infty} x(t)\,e^{-j2\pi c\,t/t_r}\,dt$	Fourier
$\ln(t/t_r)$, $t>0$	$\int_0^{\infty} x(t)\,\frac{1}{\sqrt{t}}\,e^{-j2\pi c\,\ln(t/t_r)}\,dt$	Mellin
$\mathrm{sgn}(t)\lvert t/t_r\rvert^{\kappa}$ $\kappa\neq 0$	$\int_{-\infty}^{\infty} x(t)\,\sqrt{\lvert\kappa\rvert\lvert t/t_r\rvert^{\kappa-1}}\,e^{-j2\pi c\,\mathrm{sgn}(t)\lvert t/t_r\rvert^{\kappa}}\,dt$	Power
e^{t/t_r}	$\int_{-\infty}^{\infty} x(t)\,\sqrt{e^{t/t_r}}\,e^{-j2\pi c\,e^{t/t_r}}\,dt$	Exponential

discrete dispersive model in (15). In essence, this is a generalization of the discrete narrowband SF representation in (4) [14], [15], [18] via the unitary warping relation in (10) [6]. The basic discretization procedure is to warp the output signal of the dispersive system so that it can be represented in terms of the narrowband SF of the warped system $\mathcal{L}=\mathcal{U}_\xi^{-1}\mathcal{Z}\mathcal{U}_\xi$ in Fig. 1. The warped input signal $(\mathcal{U}_\xi x)(t)$ can be shown to be essentially time-frequency limited as $x(t)$ is limited in the MST based domain.

Initially, we warp the output signal $(\mathcal{Z}x)(t)$ of the dispersive system to obtain $(\mathcal{U}_\xi\mathcal{Z}x)(t)$ that corresponds to a potential output of a unitarily equivalent narrowband system $\mathcal{L}=\mathcal{U}_\xi^{-1}\mathcal{Z}\mathcal{U}_\xi$. For notational convenience, we denote $a(\tau,\nu)\triangleq \mathrm{SF}_{\mathcal{U}_\xi\mathcal{Z}\mathcal{U}_\xi^{-1}}(\tau,\nu)e^{-j\pi\nu\tau}$ to rewrite (11) as

$$\begin{aligned}&(\mathcal{U}_\xi\mathcal{Z}x)(t)\\&=\int_{-\infty}^{\infty}\int_{-\infty}^{\infty} a(\tau,\nu)(\mathcal{U}_\xi x)(t-\tau)e^{j2\pi\nu t}d\tau d\nu\\&=\int_{-\infty}^{\infty}\int_{-\infty}^{\infty} A(f,\nu)(\mathcal{F}\mathcal{U}_\xi x)(f)e^{j2\pi ft}e^{j2\pi\nu t}df d\nu\end{aligned}\tag{18}$$

where $A(f,\nu)$ is the Fourier transform of $a(\tau,\nu)$.

Based on the assumption that $x(t)$ has a bounded support $[\lambda_0,\lambda_1]$ in the MST domain and using the relation in (14), the signal $(\mathcal{U}_\xi x)(t)$ is frequency limited within $[\lambda_0/t_r,\lambda_1/t_r]$, with bandwidth Λ/t_r. Thus, we can replace $(\mathcal{F}\mathcal{U}_\xi x)(f)$ in (18) with $(\mathcal{F}\mathcal{U}_\xi x)(f)\vartheta_{[\lambda_0/t_r,\lambda_1/t_r]}(f)$ where $\vartheta_Q(\cdot)$ is a rectangular window within the range of values defined by Q. As a result, the Fourier series expansion of $A(f,\nu)\vartheta_{[\lambda_0/t_r,\lambda_1/t_r]}(f)$ is given by

$$A(f,\nu)\vartheta_{\left[\frac{\lambda_0}{t_r},\frac{\lambda_1}{t_r}\right]}(f)=\sum_{l\in\mathbb{Z}} a_l(\nu)e^{-j2\pi\frac{l}{\Lambda}ft_r}\tag{19}$$

where the Fourier coefficient is given by

$$\begin{aligned}a_l(\nu)&=\frac{t_r}{\Lambda}\int_{\frac{\lambda_0}{t_r}}^{\frac{\lambda_1}{t_r}} A(f,\nu)e^{j2\pi\frac{l}{\Lambda}ft_r}df\\&=\frac{t_r}{\Lambda}\int_{\frac{\lambda_0}{t_r}}^{\frac{\lambda_1}{t_r}}\int_{-\infty}^{\infty} a(\tilde\tau,\nu)e^{-j2\pi\tilde\tau f}d\tilde\tau e^{j2\pi\frac{l}{\Lambda}ft_r}df\\&=\int_{-\infty}^{\infty}\mathrm{SF}_{\mathcal{U}_\xi\mathcal{Z}\mathcal{U}_\xi^{-1}}(\tilde\tau,\nu)e^{-j\pi\nu\tilde\tau}e^{j\pi\left(\frac{l}{\Lambda}-\frac{\tilde\tau}{t_r}\right)(\lambda_0+\lambda_1)}\\&\qquad\times\mathrm{sinc}\left(\left(\frac{l}{\Lambda}-\frac{\tilde\tau}{t_r}\right)\Lambda\right)d\tilde\tau.\end{aligned}\tag{20}$$

Inserting (19) into (18) and simplifying, we obtain

$$(\mathcal{U}_\xi\mathcal{Z}x)(t)=\sum_{l\in\mathbb{Z}}(\mathcal{U}_\xi x)\left(t-\frac{l}{\Lambda}t_r\right)b_l(t)\tag{21}$$

where $b_l(t)=\int_{-\infty}^{\infty}a_l(\nu)e^{j2\pi\nu t}d\nu$.

Also, as we assumed that the time-warped output signal $(\mathcal{U}_\xi\mathcal{Z}x)(t)$ is time-limited within $[t_r\gamma_0,t_r\gamma_1,]$, with time duration $t_r\Gamma$, both sides of (21) can be multiplied by $\vartheta_{[t_r\gamma_0,t_r\gamma_1]}(t)$. As a result, $b_l(t)\vartheta_{[t_r\gamma_0,t_r\gamma_1]}(t)$ can be decomposed using the Fourier expansion

$$b_l(t)\vartheta_{[t_r\gamma_0,t_r\gamma_1]}(t)=\sum_{k\in\mathbb{Z}}B_{l,k}e^{j2\pi t\frac{k}{t_r\Gamma}}\tag{22}$$

where

$$\begin{aligned}B_{l,k}&=\frac{1}{t_r\Gamma}\int_{t_r\gamma_0}^{t_r\gamma_1} b_l(t)e^{-j2\pi\frac{k}{\Gamma}\frac{t}{t_r}}dt\\&=\int_{-\infty}^{\infty}\int_{-\infty}^{\infty}\mathrm{SF}_{\mathcal{U}_\xi\mathcal{Z}\mathcal{U}_\xi^{-1}}(\tilde\tau,\tilde\nu)e^{-j\pi\tilde\nu\tilde\tau}e^{j\pi\left(\frac{l}{\Lambda}-\frac{\tilde\tau}{t_r}\right)(\lambda_0+\lambda_1)}\\&\qquad\times e^{j\pi\left(\tilde\nu t_r-\frac{k}{\Gamma}\right)(\gamma_0+\gamma_1)}\cdot\mathrm{sinc}\left((l/\Lambda-\tilde\tau/t_r)\Lambda\right)\\&\qquad\times\mathrm{sinc}\left((k/\Gamma-\tilde\nu t_r)\Gamma\right)d\tilde\tau d\tilde\nu\\&\equiv\widehat{\mathrm{DSF}}_{\mathcal{Z}}(l/\Lambda,k/\Gamma).\end{aligned}\tag{23}$$

The last equality follows from the change of variables $\tilde\tau=t_r\tilde\zeta$ and $\tilde\nu=\tilde\beta/t_r$ and the warping relation in (10). Replacing (23) into (22), and then the resulting equation into (21), yields

$$(\mathcal{U}_\xi\mathcal{Z}x)(t)=\sum_{l\in\mathbb{Z}}\sum_{k\in\mathbb{Z}}\widehat{\mathrm{DSF}}_{\mathcal{Z}}(l/\Lambda,k/\Gamma)\left(\mathcal{M}_{\frac{k}{t_r\Gamma}}\mathcal{S}_{\frac{lt_r}{\Lambda}}\mathcal{U}_\xi x\right)(t).\tag{24}$$

Note that (24) effectively decomposes the warped narrowband system $\mathcal{U}_\xi\mathcal{Z}\mathcal{U}_\xi^{-1}$ into a weighted summation of sampled time and frequency shifts, and this decomposition is actually equivalent to the discrete time-frequency model of narrowband LTV systems in (4) [14], [15], [18]. Applying $\mathcal{U}_\xi^{-1}$ to both sides

of (24), and using the fact that $\mathcal{U}_\xi^{-1}$ is a linear operator, we obtain

$$(\mathcal{Z}x)(t) = \sum_{l\in\mathbb{Z}}\sum_{k\in\mathbb{Z}} \widehat{\mathrm{DSF}}_{\mathcal{Z}}(l/\Lambda, k/\Gamma)\left(\mathcal{U}_\xi^{-1}\mathcal{M}_{\frac{k}{T}}\mathcal{S}_{\frac{l}{W}}\mathcal{U}_\xi x\right)(t).$$

This is equivalent to (15) because, using (7) and (8), we have

$$\begin{aligned}\mathcal{U}_\xi^{-1}\mathcal{M}_{\frac{k}{t_r\Gamma}}\mathcal{S}_{\frac{lt_r}{\Lambda}}\mathcal{U}_\xi &= \left(\mathcal{U}_\xi^{-1}\mathcal{M}_{\frac{k}{t_r\Gamma}}\mathcal{U}_\xi\right)\left(\mathcal{U}_\xi^{-1}\mathcal{S}_{\frac{lt_r}{\Lambda}}\mathcal{U}_\xi\right)\\ &= \mathcal{D}_{\frac{k}{\Gamma}}^{(\xi)}\mathcal{G}_{\frac{l}{\Lambda}}^{(\xi)}.\end{aligned}$$

Note that the discrete system model in (15) generalizes the narrowband system model in (4) when $\xi(t/t_r) = t/t_r$. This follows from the fact that, when $\xi(t/t_r) = t/t_r$, the unitary warping operator in (9) reduces to the identity operator, i.e., $(\mathcal{U}_\xi x)(t) = x(t)$. As a result, $\mathcal{Z} = \mathcal{U}_\xi^{-1}\mathcal{L}\mathcal{U}_\xi = \mathcal{L}$ and the simplified system is no longer dispersive. For a nonlinear function $\xi(t/t_r)$, the discrete characterization in (15) is useful in processing real-life dispersive systems as we demonstrate next.

V. Shallow Water Acoustic Transmission

In order to demonstrate the usefulness of the proposed general dispersive system characterization, we investigate its application to acoustic transmission in shallow water environments. The propagation characteristics can provide us with the specific nonlinear characteristic function $\xi(t/t_r)$ that defines the dispersion in this environment. Thus, the corresponding discrete DSF representation can be applied to exploit the potential diversity suggested by the model when the acoustic signaling is appropriately designed to match the system characteristics.

A. Dispersive Shallow Water Environment

Due to the interaction between the ocean surface and sediment, the acoustic shallow water propagation can be represented in terms of normal modes [8]. When the acoustic signal enters the shallow water waveguide, it breaks up into different modes. At each mode, different frequency components travel at different speeds. As a result, for ideal acoustic waveguides (implying free surface and perfectly rigid bottom), the group velocity at the mth mode for frequency f is given by $U_m(f) = c\sqrt{1-(f_m^2/f^2)}$, $f \geq f_m$, where c is the speed of sound in water, $f_m = mc/(2d)$ is the cutoff frequency of the mth mode, and d is the water depth. Note that at each mode, only higher frequency components $(f > f_m)$ can travel through the waveguide and the group velocity $U_m(f)$ is always less than c. At the receiver, those modes combine to constitute the output signal.

This group velocity variation for different frequencies will cause an impulse signal transmitted at time $t = 0$ through the shallow water environment to arrive at the mth mode asymptotically having a nonlinear time-varying phase[5] [8]

$$\phi(t/t_r) = \phi(t) = 2\pi f_m(t^2-\alpha^2)^{\frac{1}{2}}. \tag{25}$$

Here, R is the distance between the source and the receiver, and $\alpha = R/c$ corresponds to the propagation delay in a nondispersive environment. In highly dispersive environments such as shallow water, the slower group velocity leads to arrival times that are much greater than α. The phase in (25) was obtained assuming $t \gg \alpha$ [8]. The resulting instantaneous frequency, given by $(d/dt)\phi(t) = f_m t/(t^2-\alpha^2)^{1/2}$, demonstrates the characteristic dispersive time-frequency nature of this underwater propagation. This is further demonstrated in Fig. 2 where the instantaneous frequency is plotted for the first six modes with $c = 1{,}500$ m/s, $d = 100$ m, and $R = 30$ km. Note that these curves agree with the results obtained by time-frequency analyzing experimental data in [9].

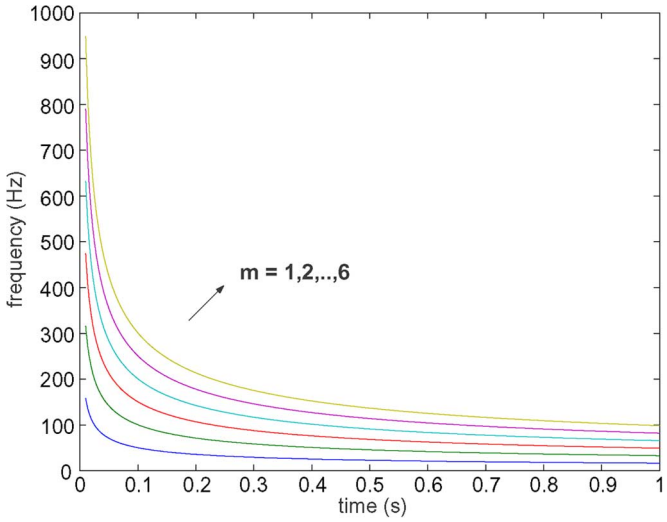

Fig. 2. Dispersive instantaneous frequency corresponding to the first six modes of $\phi(t)$ in (25).

B. Dispersive Characterization

Although the shallow water system characteristics were studied before from the group velocity perspective [8] and also experimentally tested [9], the system propagation has not yet been formulated in terms of dispersive spreading in the time-frequency plane. Thus, considering a signal $x(t)$ propagating through a shallow water environment, we next derive the DSF representation of the received signal $y(t)$, following the general dispersive model in (6).

Note that it follows from (25) that the phase changes caused by shallow water propagation are provided by the system characteristic function

$$\xi(t) = \xi_\alpha(t) = (t^2-\alpha^2)^{\frac{1}{2}}, \;\; t \gg \alpha, \quad t > 0. \tag{26}$$

Substituting (26) into (7) and (8) to compute the dispersive frequency shift and generalized time shift, respectively, we obtain the simplified signal transformations

$$\left(\mathcal{D}_\beta^{(\xi_\alpha)}x\right)(t) = \mathrm{e}^{j2\pi\frac{\beta}{t_r}\sqrt{t^2-\alpha^2}}x(t) \tag{27}$$

$$\left(\mathcal{G}_\zeta^{(\xi_\alpha)}x\right)(t) \approx \left(\mathcal{S}_{t_r\zeta}x\right)(t) = x(t-t_r\zeta). \tag{28}$$

The signal transformation in (27) is a nonlinear frequency shift due to the modal frequency dispersion. The transformation in (28) can be approximated by a constant time shift following the

[5]Without loss of generality, we often assume that the time reference $t_r = 1$ s for the rest of this paper.

assumption that $t \gg \alpha$. Specifically, the time axis transformation of the generalized time-shifted signal in (8) approximates to a time shift

$$x\left(t_r\xi_\alpha^{-1}\left(\xi_\alpha(t/t_r)-\zeta\right)\right) = x\left(\left(\sqrt{t^2-\alpha^2}-t_r\zeta\right)^2+\alpha^2\right)^{1/2} \approx x(t-t_r\zeta).$$

The amplitude variation in (8) can also be shown to simplify to unity when $t \gg \alpha$.

If we let $\beta = t_r\nu$ and $\zeta = \tau/t_r$ in (27) and (28) and then replace them in (6), then the received signal $y(t)$ can be represented as a weighted superposition of constant time shifts and dispersive frequency shifts using

$$y(t) = \int_0^{T_d}\int_0^{F_m} H(\tau,\nu)x(t-\tau)\mathrm{e}^{j2\pi\nu(t^2-\alpha^2)^{\frac{1}{2}}}\,d\nu d\tau \qquad (29)$$

where $H(\tau,\nu) = \mathrm{DSF}_{\mathcal{Z}}(\tau/t_r, t_r\nu)$ when $\xi(t) = \xi_\alpha(t)$ in (6). Note that (29) provides a meaningful physical interpretation of the propagation through the shallow water environment with dense multipath and continuous modal frequency dispersion [8]. In particular, τ and ν correspond to the multipath and cutoff frequency parameters, respectively, and the DSF $H(\nu,\tau)$ provides a measure of how the transmitted energy is distributed in the (τ,ν)-plane. In practice, since propagation loss increases with propagation distance and since higher modes suffer from more reflection loss, the DSF can be assumed to have a finite support $(\tau,\nu) \in [0,T_d]\times[0,F_m]$, where T_d is the multipath spread and F_m is the cutoff frequency for the highest mode of interest.

When the environment is randomly varying, the DSF $H(\tau,\nu)$ can be modeled as a stochastic process and a dispersive scattering function (DSC), $\varpi(\tau,\nu)$, can be defined to measure the second-order statistics of the DSF. Specifically, if the system responses at different time shifts and frequency dispersions are statistically uncorrelated, then the DSC satisfies

$$\mathrm{E}\left[H(\tau,\nu)H^*(\tau',\nu')\right] = \varpi(\tau,\nu)\delta(\nu-\nu')\delta(\tau-\tau'). \qquad (30)$$

C. Discrete Modeling for Shallow Water Acoustic Communications

We consider a shallow water acoustic communication application [22], and restrict our discussion to the single-user, binary signaling case. The ith information bit $b_i = \pm 1$ is transmitted using the signal $b_i x(t-iT)$, where $x(t)$ is the signaling waveform with symbol duration T and effective bandwidth W. Under the assumption of perfect symbol synchronization and negligible intersymbol interference ($T_d \ll T$), the ith symbol can be decoded independently. Thus, without loss of generality, we consider the reception of the first ($i=0$) symbol. The overall received signal is given by $r(t) = by(t)+n(t)$, where $b = b_0$, $y(t)$ is defined in (29), and $n(t)$ is additive white Gaussian noise.

Based on our discussion in Section IV, the sampling intervals used to discretize the (τ,ν) parameters in (29) are $\widetilde{T} = \Lambda t_r$ and $\widetilde{W} = \Gamma/t_r$, where $\widetilde{T}$ and $\widetilde{W}$ are respectively the time duration and bandwidth of the warped signal $(\mathcal{U}_{\xi_\alpha}x)(t) = (t^{1/2}/(t^2-\alpha^2)^{1/4})x((t^2-\alpha^2)^{1/2})$. However, since $t \gg \alpha$, it follows that the duration and bandwidth of $x(t)$ and $(\mathcal{U}_{\xi_\alpha}x)(t)$ are approximately the same. Thus, (29) can be decomposed[6] into a weighted summation of discrete time shifts and frequency dispersions [following our proposed discrete model in (15)] to yield

$$y(t) \approx \sum_{l=0}^{L}\sum_{k=0}^{K} \hat{H}(l/W, k/T)x_{l,k}(t). \qquad (31)$$

Here, the finite summation limits follow from the environment parameters as $L = \lceil T_d W\rceil$ and $K = \lceil F_m T\rceil$. The basic waveform

$$x_{l,k}(t) = x\left(t-\frac{l}{W}\right)\mathrm{e}^{j2\pi\frac{k}{T}(t^2-\alpha^2)^{\frac{1}{2}}} \qquad (32)$$

undergoes discrete time shifts l/W, $l = 0,\ldots,L$, as well as discrete dispersive frequency shifts $k(t^2-\alpha^2)^{1/2}/T$, $k = 0,\ldots,K$. The sampled version of the smoothed DSF is given by

$$\hat{H}\left(\frac{l}{W},\frac{k}{T}\right) = \int_0^{T_d}\int_0^{F_m} H(\tau',\nu')\mathrm{e}^{-j\pi\nu'\tau'}\mathrm{e}^{-j\pi\left(\frac{k}{T}-\nu'\right)T} \times \mathrm{sinc}(k-\nu'T)\mathrm{sinc}(l-\tau'W)\,d\nu' d\tau'. \qquad (33)$$

It can be seen that (31) effectively divides the received signal into $D = (K+1)(L+1)$ components, leading to a potential diversity system with order D. Note that D is approximately proportional to the environment's spreading factor $F_m T_d$ and the time-bandwidth product TW of the transmitted waveform. The diversity implementation can be accomplished by a joint design of the transmitted waveform and a matched RAKE receiver.

D. Waveform Signaling and RAKE Receiver Design

In order to be able to use the discrete model in (31) to improve processing performance, we need to find an appropriate waveform $x(t)$ so that a RAKE receiver can exploit the multipath-dispersion diversity inherent to the dispersive shallow water environment. As signals with high time-bandwidth product can undergo dispersions in time and frequency, we consider the use of direct sequence spread spectrum (DSSS) signals [30] as our transmitted waveform.

DSSS signals are well-suited to exploit both time and frequency diversity offered by time-varying environments [18]. In fact, DSSS systems have been used for underwater communications to exploit multipath and Doppler diversity (see for example [22], [31], and references therein). Specifically, a DSSS signal is given by $x(t) = \sum_{p=0}^{P-1} s_p g(t-pT_c)$, where s_p is the spreading sequence, T_c is the chip duration, and $g(t)$ is the chip waveform. In the case of a narrowband chip waveform, $x(t)$ has a time-bandwidth product proportional to the spreading gain P, i.e., $TW \approx T/T_c = P$.

To exploit the dispersive frequency diversity, the chip waveform can be shaped with a time-varying (TV) amplitude that depends on the characteristic function $\xi_\alpha(t)$ in (26), i.e.,

$$g(t) = \left(\xi'_\alpha(t)\right)^{-1/2} = t^{1/2}/(t^2-\alpha^2)^{1/4}. \qquad (34)$$

[6]In addition to the warping-based approach, this discrete decomposition can also be obtained using a transform-based approach, as shown in [29].

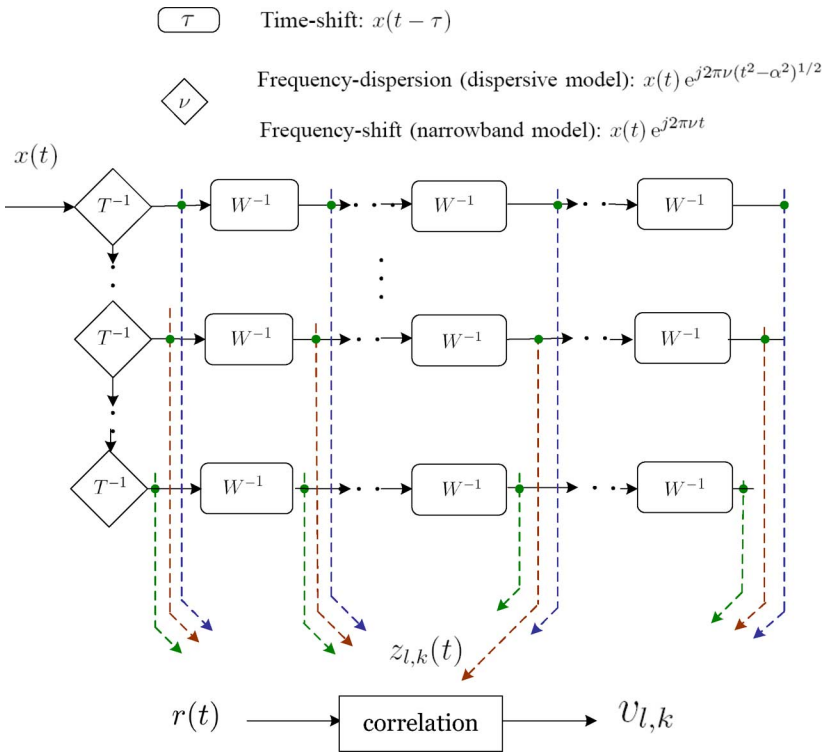

Fig. 3. Computation of the decision statistic $v_{l,k}$ in (35) in a generalized time-frequency RAKE receiver. The leftmost column performs dispersive or constant frequency shifts depending on the propagation model used.

Under the assumption $t \gg \alpha$, this TV shape can be approximated by a rectangular pulse. As we will show in Section V-E, such an approximation has very little impact on our numerical results.

After propagating through the shallow water medium, the waveform undergoes time shifts and frequency dispersions, and a RAKE receiver is needed to resolve different diversity components from the received waveform. Specifically, a generalized time-frequency RAKE receiver projects the received signal $r(t)$ onto a waveform basis $z_{l,k}(t)$ to obtain the sufficient statistics

$$v_{l,k} = \int_t r(t) z_{l,k}^*(t)dt = b s_{l,k} + n_{l,k} \tag{35}$$

where $s_{l,k} \triangleq \int_t y(t) z_{l,k}^*(t)dt$ and $n_{l,k} \triangleq \int_t n(t) z_{l,k}^*(t)dt$.

The waveform basis $z_{l,k}(t)$ in (35) are time-frequency transformed versions of the basic waveform $x(t)$. The transformations are based on the choice of the system model. For example, Fig. 3 shows a generic RAKE receiver structure for a narrowband system model and a dispersive system model. In the case of the narrowband model in (4), $z_{l,k}(t) = x(t - l/W)\mathrm{e}^{j2\pi kt/T}$ is matched to the time-frequency shifted versions of $x(t)$; if the dispersive model in (31) is used, $z_{l,k}(t) = x(t - l/W)\mathrm{e}^{j2\pi(k/T)(t^2-\alpha^2)^{1/2}}$ is matched to the time-shifted and frequency-dispersed (TSFD) version of $x(t)$. Therefore, it is important to identify the correct system model in order to specify the RAKE receiver structure that is matched to the environment characteristics.

For coherent detection, the best form of combining is the maximum ratio combining (MRC), where the sufficient statistics vector is combined in an optimal way to maximize the output signal-to-noise ratio (SNR). Specifically, the estimate of bit b is given by

$$\hat{b} = \mathrm{sign}\left\{\mathrm{Re}\left\{\sum_{l=0}^{L}\sum_{k=0}^{K} v_{l,k} s_{l,k}^*\right\}\right\} \tag{36}$$

where $\mathrm{sign}(x) = x/|x|$ if $x \neq 0$ and zero otherwise.

E. Performance Analysis

To demonstrate the importance of choosing the matched system model and waveform to obtain the desired diversity gain, we present a simple performance analysis and show numerical results using an illustrative example.

For notational convenience, we will concatenate the aforementioned waveforms or coefficients based on their time-frequency indices (l,k) into the following vectors, each of length D

$$\begin{aligned}\mathbf{H} &= [H_{0,0}, \ldots, H_{l,k}, \ldots, H_{L,K}]^{\mathbb{T}} \\ \mathbf{z}(t) &= [z_{0,0}(t), \ldots, z_{l,k}(t), \ldots, z_{L,K}(t)]^{\mathbb{T}} \\ \mathbf{x}(t) &= [x_{0,0}(t), \ldots, x_{l,k}(t), \ldots, x_{L,K}(t)]^{\mathbb{T}}\end{aligned}$$

where $\mathbb{T}$ denotes transpose. For binary signals using the MRC scheme in (36), and when the dispersive scattering function $\varpi(\tau,\nu)$ has a zero-mean, complex Gaussian distribution, and for each pair of (l,k), $z_{l,k}(t)$ has unit energy, i.e., $\int_t z_{l,k}(t)dt = 1$, the bit-error rate (BER) is given by [32]

$$P_b = \frac{1}{\pi}\int_0^{\pi/2}\prod_{d=1}^{D}\left(1 + \frac{\gamma_b \eta_d}{\sin\theta^2}\right)^{-1} d\theta. \tag{37}$$

Here, γ_b is the average SNR per bit, and η_d are the eigenvalues of the matrix

$$\mathbf{\Sigma} = \mathbf{R_{xz}} \mathbf{\Omega_H} \mathbf{R_{xz}^\dagger} \tag{38}$$

where $\dagger$ denotes Hermitian operation, $\mathbf{R_{xz}} = \int_t \mathbf{x}(t)\mathbf{z}^\dagger(t)dt$ is the cross-correlation matrix of waveform vectors $\mathbf{x}(t)$ and $\mathbf{z}(t)$, and $\mathbf{\Omega_H} = \mathrm{E}[\mathbf{H}\mathbf{H}^\dagger]$ is the correlation matrix of the coefficient vector $\mathbf{H}$ which can be evaluated using (33) and the assumption in (30). Specifically, its (i,j)th element is given by

$$\mathrm{E}\left[\check{H}_i \check{H}_j^*\right] = \int_0^{T_d}\int_0^{F_m} \varpi(\tau,\nu)\mathrm{sinc}(k_j - \nu T) \times \mathrm{sinc}(k_i - \nu T)\mathrm{sinc}(l_i - \tau W)\mathrm{sinc}(l_j - \tau W)d\nu d\tau \tag{39}$$

where $\check{H}_i$ is the ith element of vector $\mathbf{H}$, and (l_i, k_i) is the corresponding time-frequency index so that $\check{H}_i = H_{l_i,k_i}$. Note that (39) implies a double time-frequency sampling and smoothing of the dispersive scattering function.

F. Discussions and Numerical Results

It can be seen from (37) that the effective diversity order is the rank of $\mathbf{\Sigma}$ in (38). In the special case of orthonormal $\mathbf{x}(t)$ and $\mathbf{z}(t)$, $\mathbf{\Sigma}$ has the same rank as the system correlation matrix $\mathbf{\Omega_H}$. Furthermore, from (39), if $\varpi(\tau,\nu)$ is sufficiently smooth, and if after time-frequency sampling and smoothing, all D diversity components have significantly nonzero energy and are partially correlated, then the correlation matrix $\mathbf{\Omega_H}$ will have full rank D. If all these constraints for the environment and the transceiver implementation are satisfied, the diversity system can achieve full diversity of order D.

Next, for shallow water acoustic transmission, we numerically evaluate (37) using a DSSS waveform with $T = 22$ ms and an 11-length Bark code spreading sequence so that $W \approx 1$ kHz. In order to compare the performance using dispersive and narrowband propagation models, two chip waveforms and two RAKE receivers are considered. Specifically, one chip pulse is shaped with the TV amplitude as defined in (34) to match the dispersive characteristics $\xi_\alpha(t)$ in (26). The other is a rectangular pulse matched to the narrowband assumption $\xi(t) = t$. The RAKE receiver structures are shown in Fig. 3. Specifically, the TSFD RAKE receiver is constructed according to the dispersive propagation model whereas the time-shifted and frequency-shifted (TSFS) RAKE receiver is formulated according to the narrowband model. Note that the TSFD RAKE using the TV amplitude chip waveform is completely matched to the dispersive model, whereas the TSFS RAKE using the rectangular chip waveform is completely matched to the narrowband model.

For a simple illustration, we model the transmitted energy to be uniformly distributed for all delays and dispersions, i.e., $\varpi(\tau,\nu) = 1$ for $(\tau,\nu) \in [0, T_d] \times [0, F_m]$ and zero otherwise. The multipath spread is $T_d = 2$ ms, resulting in $L = \lceil T_d W \rceil = 1$. We also assume that in this shallow acoustic environment, $c = 1\,500$ m/s, $R = 30$ km, $d = 5$ m, and we consider modal dispersions up to modes 3 and 6, corresponding to the highest cutoff frequencies $F_m = 45$ and 90 Hz, respectively. As a result, $K = \lceil T F_m \rceil = 1$ and 2, leading to the highest achievable diversity order $D = 4$ and $D = 6$, respectively.

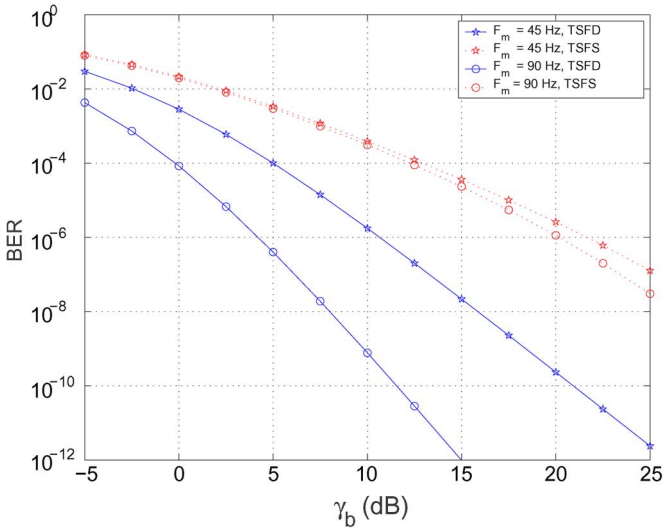

Fig. 4. Performance comparison of antipodal binary DSSS signaling with MRC RAKE receivers for shallow water acoustic transmission. The TSFD RAKE receiver assumes the model in (31), and the TSFS RAKE receiver assumes the model in (4).

Fig. 4 shows the BER performance of both RAKE receivers using two propagation models: the TSFD RAKE receiver assumes the model in (31), and the TSFS RAKE receiver assumes the model in (4). As it can be seen from the figure, larger F_m values result in better BER performance as more dispersive Doppler diversity is then exploited. The chip waveform uses a time-varying pulse shape. Note that we have also used a chip waveform with rectangular pulse shape, and we observed that the two pulse-shaped chip waveforms do not differ in BER performance for the same RAKE receiver. This is expected, as mentioned earlier, since the rectangular pulse can effectively approximate the time-varying amplitude in (34) when $t \gg \alpha$. Note, also, that for both values of F_m and both types of chip waveforms, the TSFD RAKE receiver can effectively achieve the highest diversity order D. The TSFS RAKE receiver, on the other hand, has a significant loss of diversity gain. For example, when $F_m = 45$ Hz, 10-dB more SNR is required for the TSFS RAKE receiver to achieve a 10^{-6} BER than the TSFD RAKE receiver. This result can be justified by the values of the correlation matrices $\mathbf{R_{zx}}$ of both receivers that are plotted in Fig. 5(a) and (b), respectively. As it can be observed, Fig. 5(a) shows high concentration with low sidelobes; this implies that the correlation matrix $\mathbf{R_{zx}}$ is approximately orthogonal. Also, our choices of the DSC and decomposition parameters lead to a full rank correlation matrix $\mathbf{\Omega_H}$ in (38), and, thus, we can conclude that the TSFD RAKE receiver can achieve the full diversity order D offered by the dispersive environment. On the other hand, Fig. 5(b) shows high sidelobes for the TSFS RAKE receiver, and, thus, full diversity order is not achieved when the system model is assumed narrowband.

VI. Conclusion

We proposed a new discrete framework for characterizing generalized dispersive LTV systems. This framework provides an important foundation to exploit dispersive characteristics and

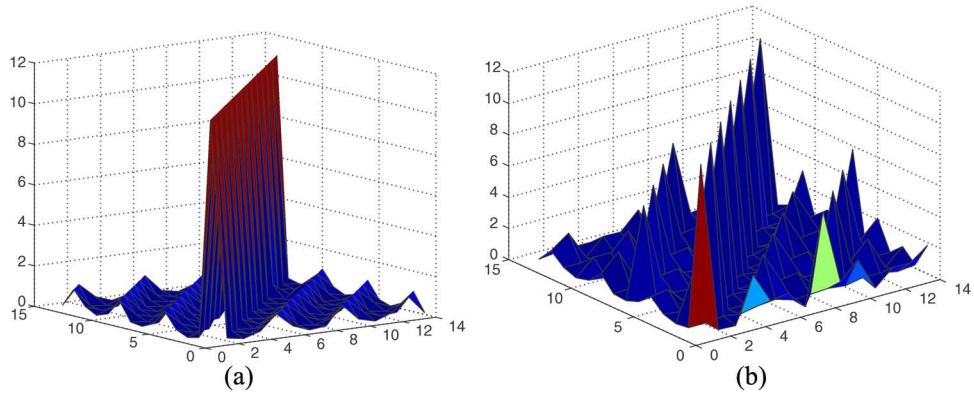

Fig. 5. Numerically computed correlation matrix $\mathbf{R_{xz}}$ in (38), where $\mathbf{x}$ is the propagation waveform vector and $\mathbf{z}$ is the RAKE waveform basis that is matched to the transmitted waveform and the assumed propagation model. (a) Transmitted DSSS waveforms with TV chip amplitude and TSFD RAKE receiver matched to the dispersive time-frequency model in (31). (b) Transmitted DSSS waveforms with rectangular chip amplitude and TSFS RAKE receiver matched to the narrowband time-frequency model in (4).

improve system performance. We base our discretization on a unitary warping relation between the narrowband and dispersive system spreading functions. This relation uses the function $\xi(t/t_r)$ to characterize the phase change on the signal caused by the dispersive system. As a result, we obtain the discrete characterization of dispersive systems as a generalization of the narrowband time-frequency model. Specifically, this discrete model decomposes the dispersive system output as a discrete representation in terms of uniformly sampled dispersive frequency shifts and generalized time shifts, weighted by a sampled and smoothed version of the dispersive spreading function. The sampling intervals of the dispersive frequency shifts and generalized time shifts are determined according to the limited bandwidth and time duration of the warped signal, specified by the function $\xi(t/t_r)$. Note that a finite approximation of the discrete representation can also be obtained depending on the support of the dispersive spreading function.

In some real-life applications, the system under consideration may be described by a function $\xi(t/t_r)$ that is noninjective or does not exist in closed form. As both of these assumptions were needed for the warping-based approach described in this paper, this approach would not be applicable to obtain the corresponding dispersive system models. When the function $\xi(t/t_r)$ is noninjective, we would need to derive the discrete model using a transform-based approach similar to the one we used in [7] for wideband system modeling and in [29] for shallow water environment modeling. Such an approach is based on how the signal is bandlimited in the time and frequency domains as a result of the signal transformations caused by the environment. We could also confine the argument of this noninjective function in a limited range of interest so that the resulting function is injective; this is similar to the causal condition we used for (26). For systems that are characterized by functions $\xi(t/t_r)$ that do not have analytical expressions, we are currently investigating different approaches on how to implement the corresponding warping transformation.

We demonstrated that our proposed discrete framework can be applied to enhance the performance of shallow water acoustic transmissions. Specifically, we identified the appropriate $\xi(t/t_r)$ for sound propagation in shallow water and showed that the generalized time shifts can be effectively reduced to constant time shifts. Thus, we obtained the discrete model for shallow water acoustic environments and investigated techniques to exploit an inherent multipath-dispersion diversity that is captured by our model. Specifically, we designed a chip waveform with time-varying amplitude to approximate orthogonal signaling for DSSS systems and a 2-D RAKE structure that is matched to the waveform and system dispersive characteristics. Numerical results demonstrate that our proposed model can outperform conventional systems that are based on narrowband models.

ACKNOWLEDGMENT

The authors would like to thank Dr. W. Kozek from Siemens, as well as the anonymous reviewers for their valuable comments that helped to improve our paper.

REFERENCES

[1] L. A. Zadeh and C. A. Desoer, *Linear System Theory: The State Space Approach*. New York: McGraw-Hill, 1963.
[2] L. J. Ziomek, *Underwater Acoustics: A Linear Systems Theory Approach*. Orlando, FL: Academic, 1985.
[3] W. Kozek, "On the transfer function calculus for underspread LTV channels," *IEEE Trans. Signal Processing*, vol. 45, no. 1, pp. 219–223, Jan. 1997.
[4] L. H. Sibul, L. G. Weiss, and T. L. Dixon, "Characterization of stochastic propagation and scattering via Gabor and wavelet transforms," *J. Comput. Acoust.*, vol. 2, no. 3, pp. 345–369, 1994.
[5] R. G. Shenoy and T. W. Parks, "The Weyl correspondence and time-frequency analysis," *IEEE Trans. Signal Process.*, vol. 42, no. 1, pp. 318–331, Feb. 1994.
[6] B. G. Iem, A. Papandreou-Suppappola, and G. F. Boudreaux-Bartels, "Wideband Weyl symbols for dispersive time-varying processing of systems and random signals," *IEEE Trans. Signal Process.*, vol. 50, no. 5, pp. 1077–1090, May 2002.
[7] Y. Jiang and A. Papandreou-Suppappola, "Discrete time-scale characterization of wideband time-varying systems," *IEEE Trans. Signal Process.*, vol. 54, no. 4, pp. 1364–1375, Apr. 2006.
[8] I. Tolstoy and C. S. Clay, *Ocean Acoustics: Theory and Experiment in Underwater Sound*. New York: McGraw-Hill, 1966.
[9] C. Chen, H. M. James, G. F. Boudreaux-Bartels, R. P. Gopu, and J. L. Colin, "Time-frequency representations for wideband acoustic signals in shallow water," in *Proc. OCEANS*, Sep. 2003, vol. 5, pp. SP2903–SP2907.

[10] A. Papandreou-Suppappola, R. L. Murray, B. G. Iem, and G. F. Boudreaux-Bartels, "Group delay shift covariant quadratic time-frequency representations," *IEEE Trans. Signal Process.*, vol. 49, no. 11, pp. 2549–2564, Nov. 2001.
[11] D. E. Newland, "Time-frequency and time-scale analysis by harmonic wavelets," in *Signal Analysis and Prediction*, A. Prochazka, Ed. Boston, MA: Birkhauser, 1998, ch. 1.
[12] M. J. Freeman, M. E. Dunham, and S. Qian, "Trans-ionospheric signal detection by time-scale representation," in *Proc. IEEE U.K. Symp. Applications of Time-Frequency and Time-Scale Methods*, Coventry, U.K., Aug. 1995, pp. 152–158.
[13] J. P. Sessarego, J. Sageloli, P. Flandrin, and M. Zakharia, "Time-frequency Wigner-Ville analysis of echoes scattered by a spherical shell," in *Wavelets, Time-Frequency Methods and Phase Space*, J. M. Combes, A. Grossman, and P. Tchamitchian, Eds. Berlin, Germany: Springer-Verlag, 1989, pp. 147–153.
[14] T. Kailath, "Sampling models for linear time-variant filters," Tech. Rep. 352, Res. Lab. Electron., Massachusetts Inst. Technol., Cambridge, May 1959.
[15] P. A. Bello, "Characterization of randomly time-variant linear channels," *IEEE Trans. Commun.*, vol. 11, no. 4, pp. 360–393, May 1963.
[16] H. Artés, G. Matz, and F. Hlawatsch, "Linear time-varying channels," Tech. Rep. 98-06, Inst. Commun. Radio Freq. Eng., Vienna Univ. Technol., Vienna, Austria, Dec. 1998.
[17] A. M. Sayeed and B. Aazhang, "Communication over multipath fading channels: A time-frequency perspective," in *Wireless Communications: TDMA vs. CDMA*. Norwell, MA: Kluwer, 1997, pp. 73–98.
[18] ——, "Joint multipath-Doppler diversity in mobile wireless communications," *IEEE Trans. Commun.*, vol. 47, no. 1, pp. 123–132, Jan. 1999.
[19] M. R. Baissas and A. M. Sayeed, "Pilot-based estimation of time-varying multipath channels for coherent CDMA receivers," *IEEE Trans. Signal Process.*, vol. 50, no. 8, pp. 2037–2049, Aug. 2002.
[20] Y. Jiang and A. Papandreou-Suppappola, "Time-scale canonical model for wideband system characterization," in *Proc. IEEE Int. Conf. Acoustic, Speech, Signal Processing*, Philadelphia, PA, Mar. 2005, vol. 4, pp. 281–284.
[21] R. Balan, H. V. Poor, S. Rickard, and S. Verdu, "Time-frequency and time-scale canonical representations of doubly spread channels," presented at the Eur. Signal Processing Conf., Vienna, Austria, Sep. 2004.
[22] F. Blackmon, E. Sozer, M. Stojanovic, and J. Proakis, "Performance comparison of RAKE and hypothesis feedback direct sequence spread spectrum techniques for underwater communication applications," in *Proc. MTS/IEEE Oceans*, Biloxi, MS, Oct. 2002, vol. 1, pp. 594–603.
[23] G. B. Folland, *Harmonic Analysis in Phase Space*. Princeton, NJ: Princeton Univ. Press, 1989.
[24] K. G. Canfield and D. L. Jones, "Implementing time-frequency representations for non-Cohen classes," presented at the 27th Asilomar Conf. Signals, Systems and Computers, Pacific Grove, CA, Nov. 1993.
[25] A. Papandreou-Suppappola, F. Hlawatsch, and G. F. Boudreaux-Bartels, "Power class time-frequency representations: Interference geometry, smoothing, and implementation," in *Proc. IEEE Signal Process. Int. Symp. Time-Frequency and Time-Scale Analysis*, Paris, France, Jun. 1996, pp. 193–196.
[26] A. Papandreou-Suppappola, B. G. Iem, R. L. Murray, and G. F. Boudreaux-Bartels, "Properties and implementation of the exponential class of quadratic time-frequency representations," in *Proc. 30th Asilomar Conf. Signals, Systems, Computers*, Pacific Grove, CA, Nov. 1996, pp. 237–241.
[27] A. Papandreou-Suppappola and S. B. Suppappola, "Sonar echo ranging using signals with non-linear time-frequency characteristics," *IEEE Signal Process. Lett.*, vol. 11, no. 3, pp. 393–396, Mar. 2004.
[28] R. G. Baraniuk and D. L. Jones, "Unitary equivalence: A new twist on signal processing," *IEEE Trans. Signal Process.*, vol. 43, no. 10, pp. 2269–2282, Oct. 1995.
[29] Y. Jiang, H. Shen, and A. Papandreou-Suppappola, "Characterization of shallow water environments with waveform design for diversity," presented at the Int. Waveform Diversity Design Conf., Lihue, HI, Jan. 2006.
[30] R. C. Dixon, *Spread Spectrum Systems*, 2nd ed. New York: Wiley, 1984.
[31] T. H. Eggen, A. B. Baggeroer, and J. C. Presig, "Communication over Doppler spread channels, Part I: Channel and receiver presentation," *IEEE J. Ocean. Eng.*, vol. 25, pp. 62–71, Jan. 2000.
[32] V. V. Veeravalli, "On performance analysis for signaling on correlated fading channels," *IEEE Trans. Commun.*, vol. 49, no. 11, pp. 1879–1883, Nov. 2001.

Ye Jiang received the B.E. and M.S. degrees in electrical engineering from Southeast University, Nanjing, China, in 1999 and 2001, respectively, and the Ph.D. degree in electrical engineering from Arizona State University, Tempe, in 2005.

From 2001 to 2005, she was a Research Assistant with Prof. A. Papandreou-Suppappola. Her research interests were in the areas of signal processing for wireless communications and time-varying system modeling. She is currently with Acoustic Technologies, Mesa, AZ.

Antonia Papandreou-Suppappola received the Ph.D. degree in electrical engineering from the University of Rhode Island, Providence, in 1995.

She held a navy-supported research faculty position. Currently, she is an Associate Professor at Arizona State University, Tempe. Her research interests are in the areas of time-frequency signal processing, integrated sensing and processing, and signal processing for wireless communications. Her publication record consists of more than 80 refereed journal articles, book chapters, and conference papers.

Dr. Papandreou-Suppappola was the recipient of the National Science Foundation CAREER Award in 2002, and she currently serves as an Associate Editor for the IEEE TRANSACTIONS ON SIGNAL PROCESSING and as the Treasurer of the Conference Board of the IEEE Signal Processing Society.